Antibody 17b Binding at the Coreceptor Site Weakens the Kinetics of the Interaction of Envelope Glycoprotein gp120 with CD4†

Wentao Zhang,‡ Alexis P. Godillot,‡ Richard Wyatt,§ Joseph Sodroski,§ and Irwin Chaiken*,‡

Department of Medicine, School of Medicine, University of Pennsylvania, Philadelphia, Pennsylvania 19104, and Department of Cancer Immunology and AIDS, Dana-Farber Cancer Institute, and Department of Pathology, Harvard Medical School, Boston, Massachusetts 02115

Received June 19, 2000; Revised Manuscript Received December 7, 2000

ABSTRACT: HIV-1 utilizes CD4 and the chemokine coreceptor for viral entry. The coreceptor CCR5 binding site on gp120 partially overlaps with the binding epitope of 17b, a neutralizing antibody of HIV-1. We designed a multicomponent biosensor assay to investigate the kinetic mechanism of interaction between gp120 and its receptors and the cooperative effect of the CCR5 binding site on the CD4 binding site, using 17b as a surrogate of CCR5. The Env gp120 proteins from four viral strains (JRFL, YU2, 89.6, and HXB2) and their corresponding C1-, V1/V2-, C5-deleted mutants (ΔJRFL, ΔYU2, Δ89.6, and ΔHXB2) were tested in this study. We found that, across the primary and lab-adapted virus strains, 17b reduced the affinity of all four full-length Env gp120s for sCD4 by decreasing the on-rate and increasing the off-rate. This effect of 17b on full-length gp120 binding to sCD4 contrasts with the enhancing effect of sCD4 on gp120−17b interaction. For the corresponding loop-deleted mutants of Env gp120, the off-rates of the gp120−sCD4 interaction were greatly reduced in the presence of 17b, resulting in higher affinities (except for that of ΔHXB2). The results suggest that, when 17b is prebound to full-length gp120, the V1/V2 loops may be relocated to a position that partially blocks the CD4-binding site, leading to weakening of the CD4 interaction. Given the fact that the 17b binding epitope partially overlaps with the binding site of CCR5, the kinetic results suggest that coreceptor CCR5 binding could have a similar "release" effect on the gp120−CD4 interaction by increasing the off-rate of the latter. The results also suggest that the neutralizing effect of 17b may arise not only from partially blocking the CCR5 binding site but also from reducing the CD4 binding affinity of gp120. This negative cooperative effect of 17b may provide insight into approaches to designing antagonists for viral entry.

Human immunodeficiency virus type-1 (HIV-1)[1] infects target cells by fusing the viral and cell membranes. The fusion process is mediated by sequential binding of virus envelope glycoprotein gp120 to the cell surface receptor CD4 (*1*−*4*) and to a specific chemokine receptor (including CCR5 and CXCR4) (*5*−*9*). A growing body of data suggests that binding of CD4 to gp120 induces conformational changes in gp120 which lead to greater exposure, or formation, of the chemokine coreceptor binding site (*10*−*13*). Coreceptor binding to gp120 is thought to cause further conformational changes in Env that result in dissociation of gp120 from the gp120−gp41 complex and further activation of gp41 (*14*−*18*). Understanding the molecular mechanisms involved in gp120−CD4−coreceptor interaction is vital to our understanding of the membrane fusion process and could help in the development of novel therapeutic approaches to combating the AIDS epidemic.

The functional activities of HIV-1 Env gp120 are related directly to its molecular structure. By comparison of the primary amino acid sequences of gp120 proteins derived from different HIV-1 isolates (*19*), the Env gp120 can be seen to contain five conserved regions (C1−C5) and five variable regions (V1−V5). The conserved regions form a core structure, which is important for the interaction of gp120 with CD4, coreceptors, and gp41 (*20*−*23*). The variable regions are more hydrophilic. The V1−V4 regions form surface-exposed looplike structures with disulfide bonds at their bases (*24*). Extensive mutational and antibody mapping studies have defined three regions recognized by broadly neutralizing antibodies in the gp120 glycoprotein: the CD4 binding site epitopes (CD4BS) (*25*−*27*), the CD4-induced epitopes (CD4i) (*12*, *22*), and the epitope for the 2G12 antibody located on the immunologically "silent" face of glycoprotein gp120 (*28*). The X-ray crystal structure of a ternary complex that includes a gp120 core, the CD4 D1D2 domain, and 17b Fab (*23*) confirms the spatial relationship between these binding epitopes (*21*). Most gp120 residues

† This work is supported by National Institutes of Health Grants PO1-GM 56550-01 and P30-AI45008 and the Structural Biology Core of the Penn Center for AIDS Research.

* To whom correspondence and reprint requests should be addressed: 909 Stellar-Chance Labs, 422 Curie Blvd., Philadelphia, PA 19104. Telephone: (215) 662-3682. Fax: (215) 349-5572. E-mail: chaiken@mail.med.upenn.edu.

‡ University of Pennsylvania.

§ Harvard Medical School.

[1] Abbreviations: AIDS, acquired immunodeficiency syndrome; CD4BS, CD4-binding site epitopes; CD4i, CD4-induced epitopes; EDC, 1-ethyl-3-[3-(dimethylamino)propyl]carbodiimide; Env, envelope protein; HIV-1, human immunodeficiency virus type 1; M-tropic, macrophage tropic; NHS, *N*-hydroxysuccinimide; PBS, phosphate-buffered saline; PDB, Protein Data Bank; sCD4, soluble CD4; SPR, surface plasmon resonance; T-tropic, T-cell tropic.

10.1021/bi001397m CCC: $20.00
Published on Web 01/19/2001

implicated in the formation of CD4i are located within or near the conserved V1−V2 stem, V3 loops, and fourth conserved (C4) region. CD4BS epitopes are sensitive to changes in several conserved gp120 regions. The mapped CD4BS and CD4i epitopes overlap with the binding sites of CD4 and the chemokine receptor, respectively, as revealed by the crystal structure (*23*). The proximity of the CD4BS and CD4i epitopes deduced from mutagenesis and structural data makes it possible that structural changes in one site influence the structure of residues in the other. Such interactions have been documented before using a cross-competition ELISA analysis of the HXB2 strain HIV-1 gp120 glycoprotein (*29*−*31*).

The monoclonal neutralizing human antibody, 17b, recognizes the CD4i epitope that partially overlaps the chemokine coreceptor CCR5 binding site (*12*, *13*, *32*). Our previous investigations have demonstrated that the rate of association of the JRFL gp120 protein with 17b is increased when CD4 is prebound to gp120 (*33*). This increased association rate results in a higher affinity of gp120 for 17b. These results support the notion that CD4-induced conformational changes in gp120 enhance gp120 binding to coreceptor CCR5, since the CCR5 binding site partially overlaps the 17b binding epitope, and therein facilitate virus entry into the cell.

To further investigate the cooperativity of the 17b and CD4 binding sites in the gp120 envelope protein, we reversed a previously configured three-component biosensor binding assay (*33*). In the current work, soluble CD4 (sCD4) was immobilized on the sensor surface. The sCD4 binding of gp120s from four viral strains (JRFL, YU2, 89.6, and HXB2) was tested in the absence and presence of 17b. Corresponding C1-, V1/V2-, C5-deleted gp120 mutants (ΔJRFL, ΔYU2, Δ89.6, and ΔHXB2) were tested in the same assay. To evaluate the CD4-induced conformational rearrangement effect on these four pairs of gp120 proteins, they were examined in the initial assay configuration, where 17b Fab was immobilized on the surface and sCD4 was the effector in the fluid phase. As reported here, these analyses have allowed us to quantitate the kinetics of a downregulation of CD4 binding induced by 17b in real time, a phenomenon which contrasts with the upregulation of 17b binding induced by CD4. We describe herein the data supporting these regulating effects and their implications for HIV cell fusion.

EXPERIMENTAL PROCEDURES

Protein Production. The human monoclonal antibody 17b, derived from an HIV-infected individual (*34*), was purified by protein A affinity chromatography. Fab fragments were produced by papain digestion of monoclonal antibodies using a commercial protocol (Pierce) as described previously (*33*).

Recombinant wild-type gp120 and the ΔC1/ΔV1/2/ΔC5 mutant (Δ82/Δ128−194/Δ492; HXBc2 numbering) were derived from the JRFL, YU2, 89.6, and HXB2 strains and were produced from stably transfected *Drosophila* Schneider 2 (S2) cell lines under the control of the metallothionein promoter as previously described (*35*). The loop-deleted mutant proteins are termed herein ΔJRFL, ΔYU2, Δ89.6, and ΔHXB2. Expressed recombinant proteins were purified by passage of gp120-containing media over an F105 Mab (anti-gp120) affinity column. After extensive washing, proteins were eluted with 100 mM glycine-HCl (pH 2.8) and immediately neutralized with 1 M Tris base. After spin concentration with Centriprep 30 spin filters (Amicon), recombinant proteins were stored at −20 °C in glycine-HCl-Tris buffer (pH 7.4) containing protease inhibitors. Soluble CD4 (sCD4) was a gift from R. Sweet (SmithKline Beecham Pharmaceuticals).

Optical Biosensor Binding Assays. Interaction analyses were performed on a BIA3000 optical biosensor (Biacore Inc.) with simultaneous monitoring of four flow cells. Immobilization of ligands (sCD4 or 17b Fab) to CM5 sensor chips was performed following the standard amine coupling procedure according to the manufacturer's specifications. Briefly, carboxyl groups on the sensor chip surface were activated by injection of 35 μL of a solution containing 0.2 M EDC and 0.05 M NHS at a flow rate of 5 μL/min. Next, the protein ligand at a concentration of ∼50 ng/mL in pH 4.5, 10 mM NaOAc buffer was passed over the chip surface at 25 °C at a flow rate of 5 μL/min until the desired number of response units for immobilized protein was reached. Then, after unreacted protein had been washed out, excess active ester groups on the sensor surface were capped by the injection of 35 μL of 1 M ethanolamine (pH 8.0) at a flow rate of 5 μL/min. A reference surface with BSA immobilized was generated at the same time under the same conditions and was used as background to correct for instrument and buffer artifacts.

Binding experiments were performed at 37 °C in PBS buffer (pH 7.4) with 0.005% Tween 20. PBS contains 10 mM phosphate and 150 mM NaCl. Association was assessed by passing gp120 solutions (the analyte in biosensor terminology) over the chip surface at a flow rate of 30 μL/min for 3 min. The concentration range for gp120 analytes was 31.2−250 nM. In the gp120−17b mixture, the molar concentration of 17b or 17b Fab was kept at a 10-fold excess over the concentration of gp120s. Excess 17b maximized the formation of the gp120−17b complex in solution. The molar concentrations of sCD4 (in the gp120−sCD4 mixtures) were kept at a 20-fold excess over the concentration of gp120s for the same reason. The gp120−17b and gp120−sCD4 mixtures were allowed to stand at room temperature for at least 1 h before injection. Dissociation of bound analytes was monitored while washing the surface with buffer for 5 min. The remaining analytes were removed with three 15 s injections of 4.5 M $MgCl_2$ at a flow rate of 100 μL/min.

RESULTS

Binding of Full-Length Glycoprotein gp120s to Immobilized sCD4 in the Absence and Presence of Antibody 17b. Optical biosensor interaction analysis was used to quantitate the effect of antibody 17b binding to HIV-1 gp120 on the subsequent interaction of gp120 with sCD4. Four gp120 variants were tested (JRFL, YU2, 89.6, and HXB2). As shown in Figure 1A, the binding assay was configured with sCD4 immobilized on the CM5 sensor chip surface. Two surface densities of sCD4, 237 and 583 RU, were generated by direct immobilization through amine coupling. The sensorgram overlays for binding of the representative case of YU2 gp120 to immobilized sCD4 (583 RU surface) in the *absence* and *presence* of 17b are shown in panels B and C of Figure 1, respectively. The signal from the reference flow cell (with BSA immobilized) was subtracted to correct for bulk effects and nonspecific binding to the surface. The

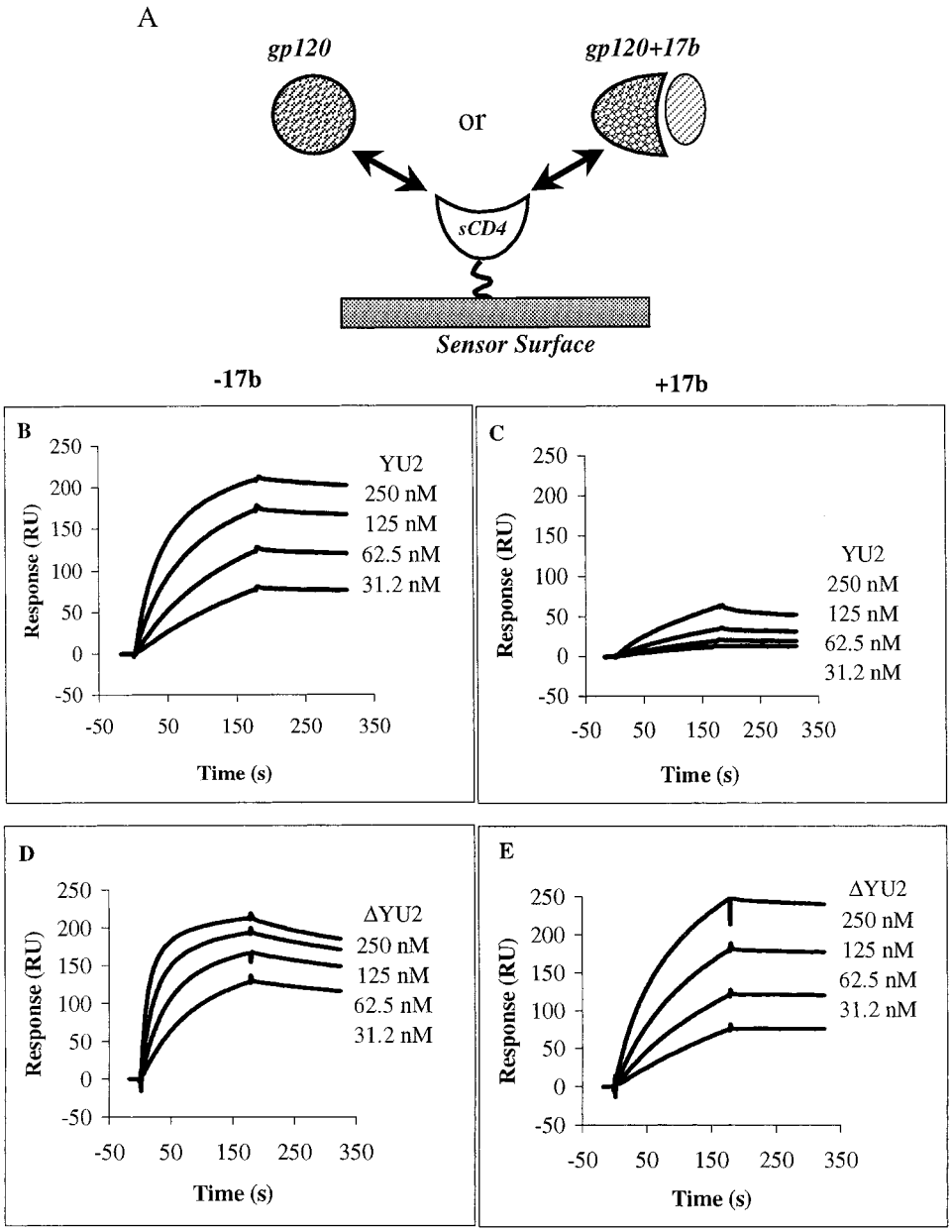

FIGURE 1: Effect of 17b on gp120−sCD4 interaction kinetics. (A) Schematic representation of the gp120−17b−sCD4 three-component biosensor configuration with sCD4 immobilized on the sensor surface. (B−E) Sensorgram overlays for binding of YU2 Env gp120 to immobilized sCD4. The surface density was 583 RU. The buffer was 10 mM phosphate (pH 7.4), 150 mM NaCl, and 0.005% P-20. The flow rate was 30 μL/min. The concentrations of gp120 proteins are shown at the right of each sensorgram. In the presence of 17b, [gp120]:[17b] = 1:10. (B and C) Full-length YU2 and (D and E) loop-deleted ΔYU2 (B and D) in the absence of 17b and (C and E) in the presence of 17b.

binding interaction was assessed over the concentration range of gp120 proteins of 31.2−250 nM. The gp120:17b molar ratio was 1:10 when 17b was present. As a control, the gp120−17b mixtures were also passed over a 17b-immobilized surface, and no binding was detected (data not shown). This result confirms that the gp120−17b complex is the predominant form in the mixture. The sensorgrams in panels B and C of Figure 1 show visually that, at the same concentration of gp120s, there is a decrease in the level of gp120 binding to sCD4 when 17b is present as indicated by the magnitude of the sensor signal. This effect is more dramatic if we consider the fact that the mass of the gp120−17b complex is twice that of gp120 alone.

The data of gp120 binding to sCD4 in the *absence* of 17b were analyzed by global analysis with a two-state conformational change model using Biaevaluation 3.1 software (Biacore Inc.). The reason for employing the two-state conformational change model to fit this set of data is that a preponderance of the data (*10*−*13*, *32*, *33*), including data from this study shown in later sections, suggests that gp120 undergoes conformational changes when it binds to sCD4. The data fit well with the two-state conformational change model ($\chi^2 < 4$). One example is shown in Figure 2A. The data for gp120 binding to sCD4 in the *presence* of 17b were analyzed by global analysis with a simple 1:1 binding model, since 17b appears to lock gp120 into a state where sCD4 no longer induces the conformational change that can be observed by this type of biosensor experiment (see Effect of 17b on Maturation of the gp120−sCD4 Complex for details). The 1:1 binding model describes this set of data

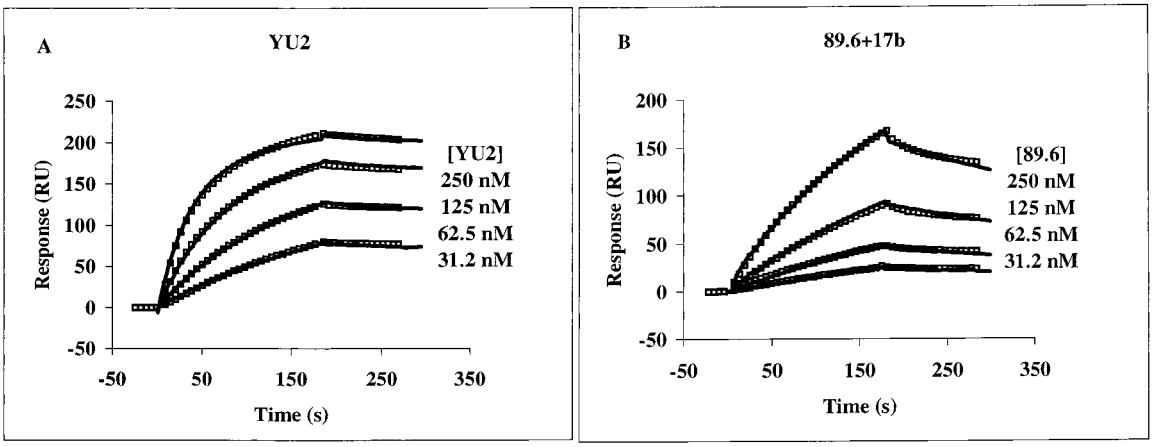

FIGURE 2: Examples of global curve-fitting analysis of binding of gp120 proteins to immobilized sCD4 (583 RU). The symbols represent the experimental data, and the lines represent the fitting results. (A) YU2 binding in the absence of 17b. The data were fit to the two-state conformational change model. (B) 89.6 binding in the presence of 17b. The data were fit to the 1:1 binding model.

Table 1: Summary of Biosensor-Derived Kinetic Constants, from Global Analysis, of the gp120−sCD4 Interaction in the Absence and Presence of 17b[a]

	without 17b[b]			with 17b[c]		
gp120	k_{on} ($\times 10^5$ M^{-1} s^{-1})	k_{off} ($\times 10^{-3}$ s^{-1})	K_d ($\times 10^{-8}$ M)	k_{on} ($\times 10^5$ M^{-1} s^{-1})	k_{off} ($\times 10^{-3}$ s^{-1})	K_d ($\times 10^{-8}$ M)
JRFL	0.866 ± 0.02	2.43 ± 0.24	2.81 ± 0.35	0.242 ± 0.004	2.33 ± 0.02	9.63 ± 0.2
YU2	1.01 ± 0.09	0.227 ± 0.04	0.225 ± 0.04	0.169 ± 0.004	1.18 ± 0.02	6.98 ± 0.2
89.6	3.26 ± 0.04	0.279 ± 0.1	0.0856 ± 0.05	0.185 ± 0.002	1.77 ± 0.01	9.57 ± 0.1
HXB2	1.01 ± 0.01	0.663 ± 0.2	0.657 ± 0.2	0.296 ± 0.005	2.00 ± 0.02	6.76 ± 0.12
ΔJRFL	0.751 ± 0.004	1.24 ± 0.01	1.65 ± 0.02	0.748 ± 0.007	0.0205 ± 0.005	0.0274 ± 0.007
ΔYU2	2.61 ± 0.02	0.716 ± 0.02	0.274 ± 0.01	0.533 ± 0.004	0.0564 ± 0.003	0.106 ± 0.007
Δ89.6	0.545 ± 0.002	2.28 ± 0.01	4.18 ± 0.02	0.320 ± 0.002	0.0543 ± 0.002	0.17 ± 0.007
ΔHXB2	6.95 ± 0.06	1.10 ± 0.05	0.158 ± 0.007	0.993 ± 0.007	0.584 ± 0.02	0.588 ± 0.02

[a] The experiments were repeated three times over two surfaces with different immobilization levels. The data from the 583 RU surface are presented here. The standard deviations were obtained from data fitting analyses. [b] In the absence of 17b, the data were fit to a two-state conformational change model:

$$A + B \underset{kd_1}{\overset{ka_1}{\rightleftharpoons}} AB^* \underset{kd_2}{\overset{ka_2}{\rightleftharpoons}} AB$$

where $k_{on} = ka_1$, $k_{off} = kd_1 * kd_2/ka_2$, and $K_d = k_{off}/k_{on}$. [c] In the presence of 17b, the data were fit to a 1:1 binding model:

$$A + B \underset{kd_1}{\overset{ka_1}{\rightleftharpoons}} AB$$

where $k_{on} = ka_1$, $k_{off} = kd_1$, $K_d = k_{off}/k_{on}$.

very well ($\chi^2 < 4$), as shown by one example in Figure 2B. The kinetic constants obtained from data analysis are summarized in Table 1 and plotted as bar graphs in Figure 3. In the *presence* of 17b, the on-rates for binding of gp120 to sCD4 are decreased dramatically (up to 17-fold) (Figure 3A), while the off-rates are increased moderately (less than 7-fold) (Figure 3B). Overall and consistently, the affinities of gp120s for sCD4 were reduced when 17b was present (up to 112-fold) (Figure 3C).

Binding of C1-, V1/V2-, C5-Deleted Mutant Glycoprotein gp120s to Immobilized sCD4 in the Absence and Presence of Antibody 17b. The C1-, V1/V2-, C5-deleted mutants (Δ82/Δ128−194/Δ492; HXBc2 numbering) are closely related to the gp120 core protein in the trimolecular complex crystal structure, except that the gp120 mutants here have intact V3 loops. These mutants contain a preserved binding site for CD4 as well as CD4BS/CD4i antibody binding epitopes despite the sequence deletions (*22*, *23*, *31*). These mutants also bind 17b. However, we know from previous work that, in the deleted form of JRFL, the cooperative linkage between the CD4 and 17b binding sites is impaired (*33*). Hence, we carried out binding experiments with ΔC1, ΔV1/V2, ΔC5 mutant glycoprotein gp120s binding to immobilized sCD4 in the *absence* and *presence* of antibody 17b, similar to the experiments described above for the full-length gp120 forms. The same biosensor surfaces as described above were used for these measurements. Sensorgram overlays for the representative case of ΔYU2-sCD4 binding on the 583 RU surface are shown in panels D and E of Figure 1. In the *presence* of 17b, binding kinetics differ from those in the absence of 17b. However, unlike the case with full-length gp120 (Figure 1B,C), affinity suppression by added 17b is not observed with the loop-deleted forms.

The data of all Δgp120 binding to sCD4 were analyzed by global analysis with a simple 1:1 binding model. The data fit well with the model ($\chi^2 < 5$). The resulting kinetic constants are summarized in Table 1 and plotted in panels D−F of Figure 3. The comparative data in Figure 3 show that 17b has a profound effect in reducing the off-rates of the Δgp120−sCD4 interaction (up to 60-fold). This resulted in an overall increase in Δgp120−sCD4 binding affinity with the exception of ΔHXB2. In the latter case, 17b does reduce the off-rate for binding to sCD4 by 2-fold, but it also reduces the on-rate by 7-fold. This results in an ~3-fold decrease in affinity.

To ensure that the 17b-induced changes in kinetics in the experiments described above were not due to the bivalency

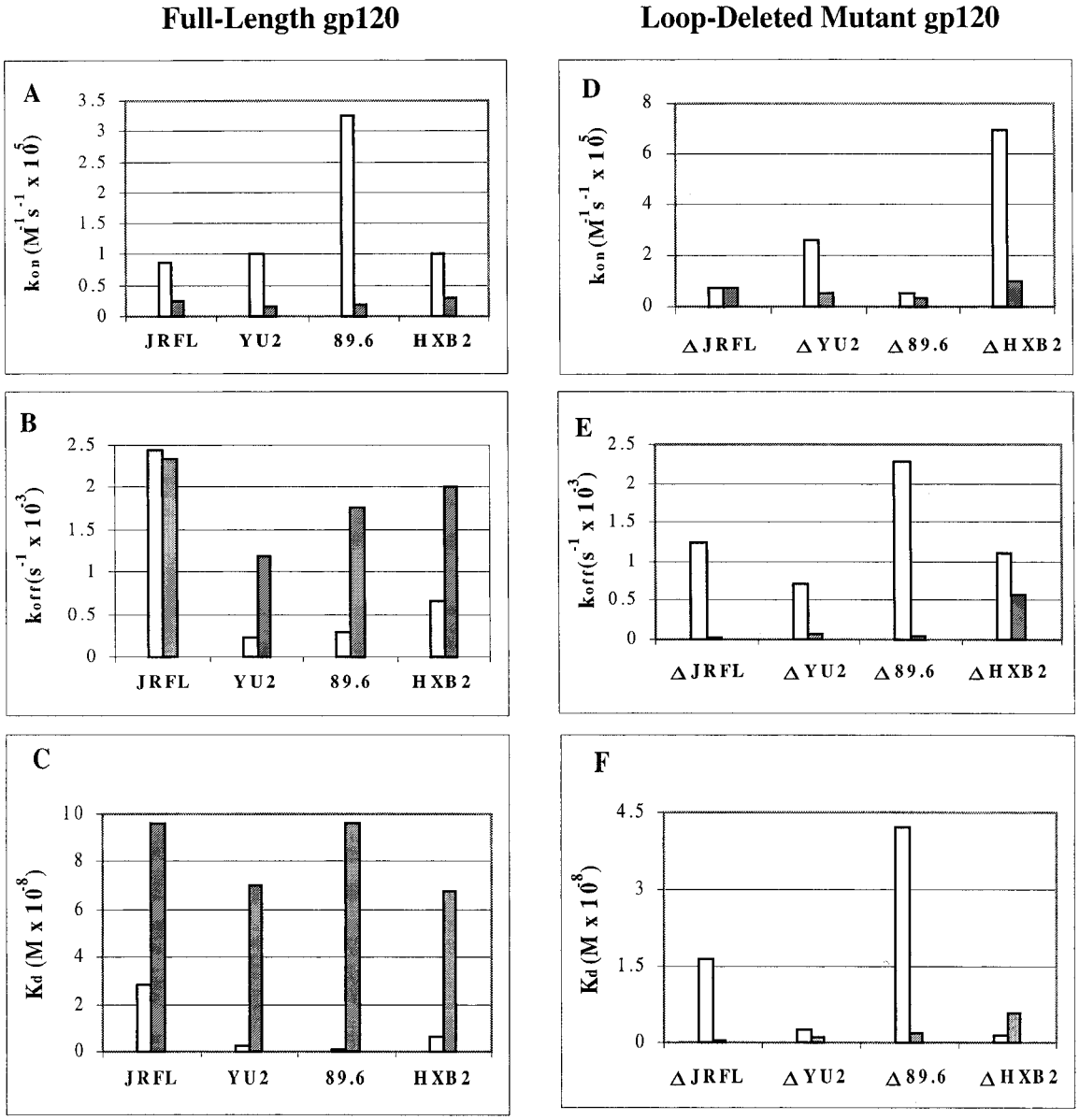

FIGURE 3: Comparison of the kinetic properties of binding of gp120 to sCD4 with or without 17b prebinding to gp120. Data are plotted for full-length (A−C) and loop-deleted (D−F) gp120 proteins: white bars, in the absence of 17b; gray bars, in the presence of 17b; (A and D) on-rate (k_{on}); (B and E) off-rate (k_{off}); and (C and F) equilibrium dissociation constant (K_d).

of the mab 17b antibody used as the analyte, a set of experiments with JRFL and ΔJRFL binding to immobilized sCD4 were performed in the *absence* and *presence* of the Fab fragment of 17b. The results that were obtained (data not shown here) were consistent with the 17b mab results, suggesting that the bivalency of the 17b mab is not a factor affecting the observed kinetics of gp120 binding to sCD4.

Effect of 17b on Maturation of the gp120−sCD4 Complex. It has been postulated that the major function of CD4 is to induce conformational changes in the Env gp120 glycoprotein that contribute to the creation, or exposure, of the binding site for the chemokine coreceptor (*10*−*13*, *21*, *32*). If the conformational rearrangements lead to a more stable (more mature) complex, and if this process takes place in a measurable time frame, the binding interaction should exhibit a slower off-rate with a longer association time. The length of the association time would induce an increasing level of maturation (increasing level of stabilization) of the complex before its dissociation in the off-process. The following experiment was designed to evaluate the relationship between association time and off-rate in the gp120−sCD4 interaction. sCD4 was directly immobilized on the sensor surface at a level of 254 RU. BSA was immobilized on the reference surface at 291 RU. Full-length JRFL (500 nM) was passed over the surfaces at a flow rate of 5 μL/min. Association times were varied from 9 to 29 min. Reference-subtracted sensorgram overlays are shown in Figure 4A. The dissociation starting point was set as 0 s. The data fit well with the two-state conformational change model ($\chi^2 < 2$). The off-rates from the curve-fitting analysis were plotted against association time (Figure 4B). The differences are small, but the trend is clear: longer association times result in slower off-rates in the absence of 17b. The same differential trends, no Δk_{off} with 17b-prebound gp120 versus k_{off} for maturation with gp120 alone, were clearly observed in two independent experiments. Interestingly, the magnitude is similar to that observed before for the binding of an antibody Fab with hen egg white lysozyme (*36*).

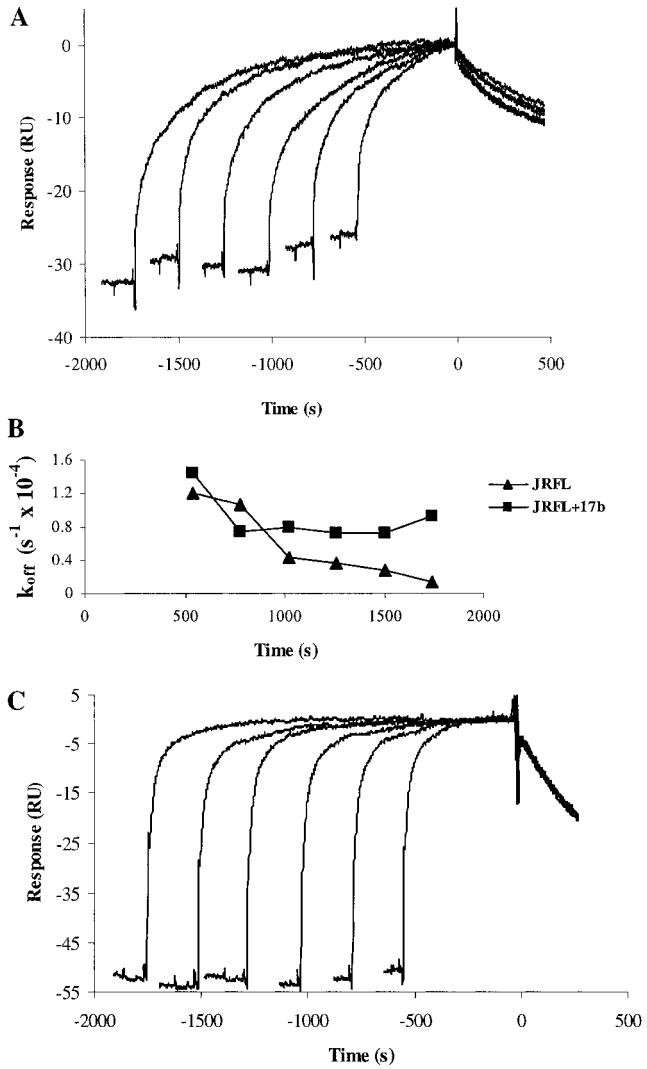

FIGURE 4: Kinetics of maturation of the gp120−sCD4 complex in the absence vs presence of 17b. (A) Sensorgram overlays of 500 nM JRFL gp120 binding to immobilized sCD4 with variable association time (from 9 to 29 min). (B) Plot of off-rate vs association time. The off-rate values were from global analysis fits to binding curves, where fits had a standard error of ≤5% in all cases. Maturation is compared for gp120 alone (sensorgram data in panel A) with results for gp120 containing prebound 17b (sensorgram data not shown). (C) Sensorgram overlays of 250 nM ΔJRFL gp120 binding to immobilized sCD4 with variable association times (from 9 to 29 min). The starting point of the dissociation phase in panels A and C is set to 0 s.

The same experiment with 500 nM JRFL was carried out in the *presence* of 17b ([JRFL]:[17b] = 1:10). As shown in Figure 4B, there is no significant trend toward slower off-rates with increasing contact times with 17b present. (The first point with the shortest contact time may reflect the fact that the association has not reached steady state.) This indicates that the 17b antibody may lock the gp120 glycoprotein into a state in which the further CD4-induced conformational changes are suppressed, at least to the extent that can be detected by this type of assay.

The loop-deleted JRFL gp120 protein mutant, ΔJRFL, was tested in the same time course with 246 and 349 RU of sCD4 and BSA, respectively, immobilized on the sensor surface. The concentration of the ΔJRFL protein was 250 nM. Figure 4C shows an overlay of the sensorgrams (after the reference subtraction) with the dissociation starting point set to 0 s. Clearly, the off-rate remains the same regardless of the association time ($k_{off} = 1.3 \times 10^{-3}$ s^{-1}). This result suggests that the variable V1/V2 loops in gp120 are involved in the conformational isomerization process when gp120 binds to CD4. Repositioning V1/V2 loops, by CD4 binding, is viewed as enhancing formation or exposure of the coreceptor binding site, leading to higher 17b binding affinity (see the next section). In addition to the movement of the V1/V2 loops, CD4 binding may introduce additional structural changes in the gp120 core. However, these would not be directly detectable in this maturation biosensor assay.

Binding of gp120s (Full-Length Proteins and Loop-Deleted Mutants) to Immobilized 17b Fab in the Absence and Presence of sCD4. Previously, we studied the binding of JRFL and ΔJRFL to immobilized 17b Fab in the *absence* and *presence* of sCD4 and found that prebinding of CD4 increases their affinity for 17b (*33*). In the view of the data obtained in this study (Figure 1 and Table 1) showing that the 17b effect on gp120−CD4 binding is not the simple reversal of the sCD4 effect on gp120−17b binding, we extended the investigation of the sCD4 effect on gp120−17b binding to include all gp120 proteins discussed above. The loop-deleted mutants also allowed us to study the role of the V1/V2 loops in the three-way interaction. The immobilization level of 17b Fab was 215 RU. The reference surface was activated by NHS/EDC and blocked by ethanolamine. The concentrations of gp120s range from 15.6 to 250 nM in the *absence* of sCD4 and from 6.25 to 100 nM in the *presence* of sCD4. We lowered the gp120 concentration when sCD4 was present, since we expected an increase in binding affinity. The binding experiments were carried out at 37 °C with a flow rate of 30 μL/min. One example of the sensorgram overlays after background correction for 89.6 and Δ89.6 is shown in Figure 5.

All the data were analyzed by global fitting with a simple 1:1 binding model ($\chi^2 < 4$). The resulting kinetic constants are summarized in Table 2. The results are consistent with our previous finding for JRFL that sCD4 enhances the binding affinity of gp120s (both full-length and loop-deleted mutants) for 17b Fab primarily by increasing the on-rates (up to 17-fold). Loop deletion alone has a moderate effect on gp120 binding to 17b in the *absence* of sCD4. Both the on-rate and off-rate for loop-deleted mutants are increased (up to 6-fold) except for that for Δ89.6. This increase results in a <3-fold increase in overall affinity. In the *presence* of sCD4, the 17b binding affinities of full-length and loop-deleted mutant gp120 are very close. These results reinforce the view that CD4-induced conformational changes involve the repositioning of the V1/V2 loops and subsequent changes in the gp120 core which create, expose, or stabilize the coreceptor binding site on gp120 and facilitate fusion.

DISCUSSION

The HIV-1 envelope glycoprotein gp120 uses CD4 and chemokine receptors such as CCR5 and CXCR4 as primary receptors in the process of virus entry into target cells. Much evidence suggests that CD4 binding induces conformational changes, in the gp120 glycoprotein, that increase the affinity of binding of gp120 to the chemokine coreceptor (*10*, *11*, *13*, *22*, *30*, *32*). The aim of this study was to gain increased insight into the interaction mechanism involving gp120, CD4,

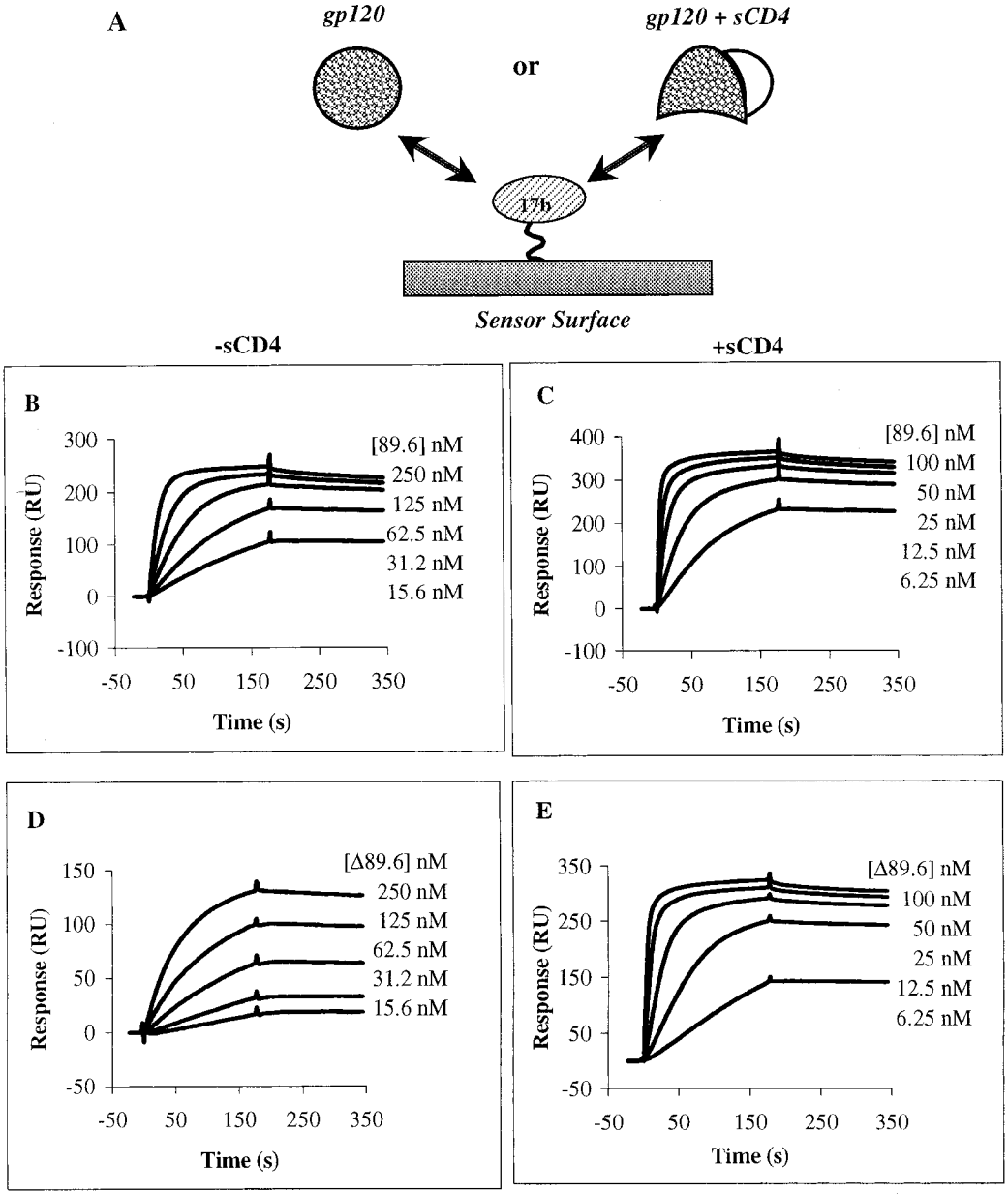

FIGURE 5: Effect of sCD4 on gp120−17b interaction kinetics. (A) Schematic representation of the gp120−17b−sCD4 three-component biosensor configuration with 17b immobilized on the sensor surface. (B−E) Sensorgram overlays for binding of 89.6 gp120 proteins to immobilized 17b Fab in the presence and absence of prebound sCD4. The surface density was 215 RU. The buffer was 10 mM phosphate (pH 7.4), 150 mM NaCl, and 0.005% P-20. The flow rate was 30 μL/min. Panels B and D depict data recorded in the absence of sCD4. Panels C and E depict data recorded in the presence of sCD4. The concentrations of gp120 proteins are shown at the right of each sensorgram. In the presence of sCD4, [gp120]:[sCD4] = 1:20.

and coreceptor binding and, furthermore, to investigate how coreceptor binding might affect the interaction kinetics of the gp120−CD4 complex. The neutralizing gp120 antibody, 17b, which binds to CD4i epitopes that partially overlap the CCR5-binding site, was used as a surrogate of CCR5 in this study.

A major finding of this work is that 17b weakens the interaction of gp120 (both primary and lab-adapted isolates) with sCD4 by decreasing the on-rate and increasing the off-rate. The overall 17b-induced affinity suppression of gp120 for sCD4 has been observed before in cross-competition ELISA analysis with the gp120 of the HXB2 isolate (*30*). The current data show that both on- and off-rates are altered in this process. This contrasts with the enhanced binding of gp120 to 17b when sCD4 is prebound. There is no direct interaction between sCD4 and 17b (data not shown). The results argue that the CD4-binding site and 17b-binding epitopes (overlapping the CCR5-binding site), while spatially distant in the gp120 molecule as revealed by the crystal structure (*23*), nonetheless influence each other with respect to the interaction mechanism. The data in this current work suggest to us the possibility that the 17b prebound form is not the same as the CD4 prebound form, which contains an upregulated 17b binding site. Since the 17b binding site is flanked by V1/V2 and V3 loops, it may be surmised that reordering of those loops in the 17b-bound form may be a factor in downregulating sCD4 binding. This view argues for a hierarchy in recognition processes involving the HIV-1 envelope, at least in solution. Hence, the first binding event appears to affect subsequent binding events, likely by

Table 2: Summary of Biosensor-Derived Kinetic Constants, from Global Analysis, of the gp120−17b Fab Interaction in the Absence and Presence of sCD4[a]

	without sCD4			with sCD4		
gp120	k_{on} ($\times 10^5$ M^{-1} s^{-1})	k_{off} ($\times 10^{-4}$ s^{-1})	K_d ($\times 10^{-10}$ M)	k_{on} ($\times 10^5$ M^{-1} s^{-1})	k_{off} ($\times 10^{-4}$ s^{-1})	K_d ($\times 10^{-10}$ M)
JRFL	0.216 ± 0.002	0.556 ± 0.1	25.7 ± 5	3.18 ± 0.02	0.645 ± 0.03	2.03 ± 0.08
YU2	0.959 ± 0.003	0.988 ± 0.06	10.3 ± 0.3	4.02 ± 0.03	0.517 ± 0.05	1.29 ± 0.1
89.6	2.68 ± 0.001	2.70 ± 0.03	10.1 ± 0.1	20.5 ± 0.1	1.98 ± 0.05	0.965 ± 0.02
HXB2	0.926 ± 0.003	2.39 ± 0.03	25.8 ± 0.3	9.13 ± 0.03	2.39 ± 0.04	2.62 ± 0.04
ΔJRFL	0.798 ± 0.003	1.41 ± 0.03	17.7 ± 0.3	13.7 ± 0.08	1.83 ± 0.06	1.34 ± 0.05
ΔYU2	1.26 ± 0.004	1.45 ± 0.03	11.5 ± 0.3	15.0 ± 0.08	1.47 ± 0.06	0.978 ± 0.04
Δ89.6	0.692 ± 0.002	1.44 ± 0.02	20.8 ± 0.3	13.8 ± 0.09	1.90 ± 0.0003	1.37 ± 0.01
ΔHXB2	5.68 ± 0.003	6.86 ± 0.06	12.1 ± 0.1	31.1 ± 0.2	3.60 ± 0.02	1.16 ± 0.02

[a] The experiments were repeated two times over two surfaces with different immobilization levels. The data from the 215 RU surface are presented here. The standard deviations were obtained from data fitting analyses. All the data were fit to the 1:1 binding model:

$$A + B \underset{kd_1}{\overset{ka_1}{\longleftrightarrow}} AB$$

where $k_{on} = ka_1$, $k_{off} = kd_1$, $K_d = k_{off}/k_{on}$.

conformational isomerization within the molecule that alters the position of the loops, in particular the V1/V2 loop.

The V1/V2 loop-deleted mutants of gp120 bind to CD4 with higher affinity in the presence of 17b, mainly due to a decrease in the dissociation rate. This result is consistent with the observation that the CD4 D1D2−gp120 core−17b Fab complex is stable enough to be crystallized (*23*). The stabilization of CD4 binding by 17b in the V1/V2 loop-deleted gp120 forms suggests that the weaker CD4 affinity of full-length gp120 in the presence of 17b could arise from the repositioning of the V1/V2 loops by 17b binding, a process which could cause partial blockage of the CD4 binding site. However, since CD4 binding and 17b binding have a nonreciprocal effect versus each other, physical movement of V1/V2 loops may not be the only structural change during the CD4−gp120−17b three-way binding process. The conformational changes may involve other structural elements in the core gp120 protein.

We used a maturation biosensor assay to evaluate the time dependence of the 17b effect on the gp120−sCD4 dissociation rate. The gp120−CD4 complex maturation data show that CD4-induced conformational change in gp120 leads to higher CD4 affinity. However, when 17b was prebound, this effect is negligible. These data support a view that the gp120 molecule is more rigid, with weaker CD4 affinity, in the presence of 17b. A possible caveat of the maturation biosensor experiment is that the more sterically hindered CD4 binding sites in the dextran hydrogel on the sensor surface may become available with longer association time, resulting in more binding of gp120. And, since the gp120−17b complex is bigger in size than free gp120, it would be harder for the gp120−17b complex to reach the hindered sites. However, the data from the smaller loop-deleted mutant, ΔJRFL, which does not show association time dependence, argue against a hindered site explanation.

The downregulation of CD4 binding by 17b suggests that the neutralizing activity of 17b could arise from both blocking CCR5 binding and weakening CD4 binding of gp120. Since there are overlaps between the 17b epitope and CCR5 binding site, 17b downregulation of CD4 binding may also imply that CCR5 binding could downregulate CD4 binding during the fusion process. This implication suggests the possibility that small molecule or peptide mimetics of 17b, possibly based on the crystal structure of the CD4−gp120−17b Fab complex, may represent a feasible approach to further investigating the cooperative mechanism involved in CD4−gp120−coreceptor binding and exploring new structure-based HIV antagonists. Toward these ends, it will be important to conduct future studies of HIV-1−receptor cooperativity in the context of the virion envelope glycoprotein complex and the receptors on the target cell membrane.

ACKNOWLEDGMENT

We thank Dr. Raymond Sweet of SmithKline Beecham Pharmaceuticals for the availability of soluble CD4 and Dr. James Robinson of Tulane University Medical Center for the availability of monoclonal antibody 17b. We thank Drs. Wayne Hendrickson and Peter Kwong of Columbia University for their helpful comments during the course of this work and Dr. Gabriela Canziani for assistance with biosensor data analyses. We also thank Dr. Cynthia Dowd of the University of Pennsylvania for her thoughtful reading and suggestions on the manuscript.

REFERENCES

1. Allan, J. S., Coligan, J. E., Barin, F., McLane, M. F., Sodroski, J. G., Rosen, C. A., Haseltine, W. A., Lee, T. H., and Essex, M. (1985) *Science 228*, 1091−4.
2. Dalgleish, A. G., Beverley, P. C., Clapham, P. R., Crawford, D. H., Greaves, M. F., and Weiss, R. A. (1984) *Nature 312*, 763−7.
3. Klatzmann, D., Champagne, E., Chamaret, S., Gruest, J., Guetard, D., Hercend, T., Gluckman, J. C., and Montagnier, L. (1984) *Nature 312*, 767−8.
4. Wyatt, R., and Sodroski, J. (1998) *Science 280*, 1884−8.
5. Moore, J. P. (1997) *Science 276*, 51−2.
6. Feng, Y., Broder, C. C., Kennedy, P. E., and Berger, E. A. (1996) *Science 272*, 872−7.
7. Doranz, B. J., Rucker, J., Yi, Y., Smyth, R. J., Samson, M., Peiper, S. C., Parmentier, M., Collman, R. G., and Doms, R. W. (1996) *Cell 85*, 1149−58.
8. Clapham, P. R., and Weiss, R. A. (1997) *Nature 388*, 230−1.
9. Dragic, T., Litwin, V., Allaway, G. P., Martin, S. R., Huang, Y., Nagashima, K. A., Cayanan, C., Maddon, P. J., Koup, R. A., Moore, J. P., and Paxton, W. A. (1996) *Nature 381*, 667−73.
10. Sattentau, Q. J., and Moore, J. P. (1991) *J. Exp. Med. 174*, 407−15.
11. Sattentau, Q. J., Moore, J. P., Vignaux, F., Traincard, F., and Poignard, P. (1993) *J. Virol. 67*, 7383−93.

12. Thali, M., Moore, J. P., Furman, C., Charles, M., Ho, D. D., Robinson, J., and Sodroski, J. (1993) *J. Virol. 67*, 3978−88.
13. Trkola, A., Dragic, T., Arthos, J., Binley, J. M., Olson, W. C., Allaway, G. P., Cheng-Mayer, C., Robinson, J., Maddon, P. J., and Moore, J. P. (1996) *Nature 384*, 184−7.
14. Weissenhorn, W., Dessen, A., Harrison, S. C., Skehel, J. J., and Wiley, D. C. (1997) *Nature 387*, 426−30.
15. Tan, K., Liu, J., Wang, J., Shen, S., and Lu, M. (1997) *Proc. Natl. Acad. Sci. U.S.A. 94*, 12303−8.
16. Lu, M., Blacklow, S. C., and Kim, P. S. (1995) *Nat. Struct. Biol. 2*, 1075−82.
17. Chan, D. C., Fass, D., Berger, J. M., and Kim, P. S. (1997) *Cell 89*, 263−73.
18. Caffrey, M., Cai, M., Kaufman, J., Stahl, S. J., Wingfield, P. T., Covell, D. G., Gronenborn, A. M., and Clore, G. M. (1998) *EMBO J. 17*, 4572−84.
19. Starcich, B. R., Hahn, B. H., Shaw, G. M., McNeely, P. D., Modrow, S., Wolf, H., Parks, E. S., Parks, W. P., Josephs, S. F., Gallo, R. C., et al. (1986) *Cell 45*, 637−48.
20. Wyatt, R., Desjardin, E., Olshevsky, U., Nixon, C., Binley, J., Olshevsky, V., and Sodroski, J. (1997) *J. Virol. 71*, 9722−31.
21. Wyatt, R., Kwong, P. D., Desjardins, E., Sweet, R. W., Robinson, J., Hendrickson, W. A., and Sodroski, J. G. (1998) *Nature 393*, 705−11.
22. Rizzuto, C. D., Wyatt, R., Hernandez-Ramos, N., Sun, Y., Kwong, P. D., Hendrickson, W. A., and Sodroski, J. (1998) *Science 280*, 1949−53.
23. Kwong, P. W. R., Robinson, J., Sweet, R. W., Sodroski, J., and Hendrickson, W. A. (1998) *Nature 393*, 648−59.
24. Leonard, C. K., Spellman, M. W., Riddle, L., Harris, R. J., Thomas, J. N., and Gregory, T. J. (1990) *J. Biol. Chem. 265*, 10373−82.
25. Ho, D. D., McKeating, J. A., Li, X. L., Moudgil, T., Daar, E. S., Sun, N. C., and Robinson, J. E. (1991) *J. Virol. 65*, 489−93.
26. Posner, M. R., Elboim, H. S., Tumber, M. B., Wiest, P. M., and Tibbetts, L. M. (1991) *Hum. Antibodies Hybridomas 2*, 74−83.
27. Thali, M., Furman, C., Ho, D. D., Robinson, J., Tilley, S., Pinter, A., and Sodroski, J. (1992) *J. Virol. 66*, 5635−41.
28. Trkola, A., Purtscher, M., Muster, T., Ballaun, C., Buchacher, A., Sullivan, N., Srinivasan, K., Sodroski, J., Moore, J. P., and Katinger, H. (1996) *J. Virol. 70*, 1100−8.
29. Binley, J. M., Wyatt, R., Desjardins, E., Kwong, P. D., Hendrickson, W., Moore, J. P., and Sodroski, J. (1998) *AIDS Res. Hum. Retroviruses 14*, 191−8.
30. Moore, J. P., and Sodroski, J. (1996) *J. Virol. 70*, 1863−72.
31. Wyatt, R., Moore, J., Accola, M., Desjardin, E., Robinson, J., and Sodroski, J. (1995) *J. Virol. 69*, 5723−33.
32. Wu, L., Gerard, N. P., Wyatt, R., Choe, H., Parolin, C., Ruffing, N., Borsetti, A., Cardoso, A. A., Desjardin, E., Newman, W., Gerard, C., and Sodroski, J. (1996) *Nature 384*, 179−83.
33. Zhang, W., Canziani, G., Plugariu, C., Wyatt, R., Sodroski, J., Sweet, R., Kwong, P., Hendrickson, W., and Chaiken, I. (1999) *Biochemistry 38*, 9405−16.
34. Willey, R. L., Martin, M. A., and Peden, K. W. (1994) *J. Virol. 68*, 1029−39.
35. Culp, J. S., Johansen, H., Hellmig, B., Beck, J., Matthews, T. J., Delers, A., and Rosenberg, M. (1991) *Bio/Technology 9*, 173−7.
36. Lipschultz, C. A., Li, Y., and Smith-Gill, S. (2000) *Methods 20*, 310−8.

BI001397M